

Nitrification of archaeal ammonia oxidizers in a high temperature hot spring

S. Chen, X.-T. Peng, H.-C Xu, and K.-W. Ta¹

Institute of Deep-sea Science and Engineering, Chinese Academy of Sciences, Sanya 572000, China

*Correspondence to: X. Peng (xtpeng@sidsse.ac.cn)

Abstract

The oxidation of ammonia by microbes has been shown to occur in diverse natural environments. However, it remains poorly understood about the link of *in situ* nitrification activity to taxonomic identities of ammonia oxidizers in high-temperature environments. Here, we studied *in situ* ammonia oxidation rates and the diversity of ammonia-oxidizing archaea (AOA) in surface and bottom sediments at 77°C in the Gongxiaoshe hot spring, Tengchong, Yunnan, China. The *in situ* ammonia oxidation rates measured by the ¹⁵N-NO₃⁻ pool dilution technique in the surface and bottom sediments were 4.80 and 5.30 nmol N g⁻¹h⁻¹, respectively. Real-time quantitative PCR (qPCR) indicated that the archaeal 16S rRNA genes and *amoA* genes were present in the range of 0.128 to 1.96 × 10⁸ and 2.75 to 9.80 × 10⁵ gene copies g⁻¹ sediment, respectively, while bacterial *amoA* was not detected. Phylogenetic analysis of 16S rRNA genes showed high sequence similarity to thermophilic ‘*Candidatus Nitrosocaldus yellowstonii*’, which represented the most abundant operational taxonomic units (OTU) in both surface and bottom sediments. The archaeal predominance was further supported by fluorescence *in situ* hybridization (FISH) visualization. The cell-specific rate of ammonia oxidation was estimated to range from 0.410 to 0.790 fmol N archaeal cell⁻¹ h⁻¹, higher than those in the two US Great Basin hot springs. These results suggest the importance of archaeal rather than bacterial ammonia oxidation in driving the nitrogen cycle in terrestrial geothermal environments.

30 **1 Introduction**

31 Nitrogen is a key element controlling the species composition, diversity, dynamics, and
32 functioning of many ecosystems (Vitousek et al., 1997). Despite of recent processes in our
33 understanding of nitrogen cycling activities in soils, fresh and marine waters, and sediments
34 (Francis et al., 2005; He et al., 2007; Beman et al., 2008; Jia and Conrad., 2009; Konneke et
35 al., 2005; Nicol and Schleper, 2006), gaps in knowledge associated with high-temperature
36 ecosystems have prevailed (Zhang et al., 2008a). Recently, some studies have elucidated
37 nitrogen metabolism and cycling in high-temperature hot spring ecosystems (Dodsworth et al.,
38 2011b; Nishizawa et al., 2013; Gerbl et al., 2014). In such systems, there has been evidence of
39 microbial communities oxidizing ammonia, the first and rate-limiting step of nitrification
40 (Reigstad et al., 2008; Hatzenpichler et al., 2008). Since the occurrence of a putative archaeal
41 *amoA* gene in hot spring environments was first reported by Weidler et al. (2007) and Spear et
42 al. (2007), thaumarchaeota possessing ammonia monooxygenase (AMO) have been obtained
43 from some terrestrial hot springs in the USA, China and Russia (Pearson et al., 2008; Zhang et
44 al., 2008a).

45 Previous studies targeting ammonia oxidation in hot springs mainly focused on archaeal
46 *amoA* gene (AOA) via a variety of culture-independent approaches (e.g. 16S rRNA clone
47 library, biomarkers) (Weidler et al., 2007; Francis et al., 2007; Zhang et al., 2008a; Jiang et al.,
48 2010; Xie et al., 2014). The results from these studies suggested that ammonia-oxidizing
49 archaea (AOA) may be ubiquitous in high-temperature environments and even more abundant
50 than their bacterial counterparts, which has led to a hypothesis that Archaea rather than
51 Bacteria drive ammonia oxidation in high-temperature hot spring environments. This
52 hypothesis, however, still needs to be verified. Currently, our knowledge about the activity of
53 AOA in such high-temperature environments is largely constrained, especially due to the data
54 deficiency of ammonia oxidation rates (Reigstad et al., 2008; Dodsworth et al., 2011b; Li et al.,
55 2015). *In situ* incubation experiments are urgently required to verify the potential activity of
56 AOA and their contribution to ammonia oxidation in such high-temperature environments.

57 In this study, we selected the Gongxiaoshe hot spring at Tengchong Geothermal Field as a
58 representative site to test the hypothesis that Archaea rather than Bacteria drive ammonia
59 oxidation in high-temperature hot spring environments. The reasons for choosing the

60 Gongxiaoshe hot spring as the research site are: 1) Ammonia concentration in the
61 Gongxiaoshe hot spring water is $102.61 \mu\text{g L}^{-1}$, thermodynamically favorable to ammonia
62 oxidation (Shock et al., 2005); 2) Ammonia-oxidizing archaea “*Candidatus Nitrosocaldus*
63 *yellowstonii*” were dominant in the hot spring water and no AOB *amoA* genes were detected
64 in the hot spring (Hou et al., 2013), indicating that the ammonia oxidation driven by Archaea
65 might be active. Here, in combination of culture-independent (fluorescence *in situ*
66 hybridization, quantitative PCR and clone library) and culture-dependent (^{15}N pool dilution
67 technique) approaches, we provide direct evidences that AOA are indeed responsible for the
68 major portion of ammonia oxidation in high-temperature hot spring environments.

69

70 **2 Materials and methods**

71 **2.1 Site description and chemical measurements**

72 Gongxiaoshe hot spring is a small pool with a diameter of ~300 cm and a depth of ~130 cm
73 (Fig. 1). Hot spring water in the pool is well mixed and water chemistry shows no difference
74 in different areas of the pool (Zhang et al., 2008b). Sediments of Gongxiaoshe hot spring are
75 found to be only present at the margin of the pool and at the bottom of the pool, representing
76 two typically sedimentary environments in this pool. The samples from the pool margins and
77 sediments from the bottom of the spring, designated SS (Surface Sediments) and BS (Bottom
78 Sediments), respectively, were collected using sterile equipment in April 2013. During
79 transportation, all of the samples were packed with dry ice. They were then stored in a freezer
80 at $-80\text{ }^{\circ}\text{C}$ in lab for further analysis.

81 Temperature and pH were measured *in situ* in the hot water spring. Temperature was
82 determined with an iButton thermometer (DS1922T, Dallas Semiconductor, USA). The pH
83 was measured using a pH Meter (SevenGo™ pH meter SG2, Mettler Toledo, USA). Water
84 samples for cation and anion analysis were filtered through a syringe filter with a $0.22 \mu\text{m}$
85 filtration membrane; these samples were diluted 10 times with deionized water and stored in
86 100 mL polypropylene bottles in the field because an analysis was carried out after two days.
87 The cation concentrations were determined using an IRIS Advantage ICP-AES, whereas the

88 anion (F^- , SO_4^{2-} , Cl^-) concentrations were determined using the Ion Chromatography System
89 (DIONEX ICS-1500, Thermo Scientific, USA). The HCO_3^- concentration was measured using
90 the Gran titration method (Appelo and Postma, 1996). The NH_4^+ -N and NO_3^- -N concentrations
91 were determined using a Nutrient Analyzer (Micromac 1000, Partech, UK).

92 2.2 ^{15}N stable isotope tracing of nitrification activity

93 Gross N nitrification rates were determined *in situ* by the ^{15}N pool dilution technique. All of
94 the nitrification measurements were conducted in 500 mL polycarbonate culture flasks
95 (Nalgene) with a silicone plug that contained 400 mL of mud (~1/3 sediment by volume). Two
96 subsamples were collected from the bottom and surface sediments with 350 μL of $K^{15}NO_3$
97 ($485 \mu mol L^{-1}$, at 10% ^{15}N). For each sample, two experiments were conducted to measure the
98 *in situ* nitrification activity: A1 (SS slurry + $^{15}NO_3^-$) and A2 (BS slurry + $^{15}NO_3^-$). Meanwhile,
99 potential nitrification activity was determined in the presence of high ammonium
100 concentration: B1 (SS slurry + $^{15}NO_3^-$ + $^{14}NH_4^+$) and B2 (BS slurry + $^{15}NO_3^-$ + $^{14}NH_4^+$). Two
101 pairs of duplicate reactors were set up in four experiments. The reactors were incubated near
102 the *in situ* conditions of the hot spring water at 77 °C for 30 and 120 min. At certain time
103 intervals (e.g., 30 min, 120 min), 80 mL aliquots were collected from the experimental
104 reactors with sterile serological pipettes and transferred to acid-cleaned 250 mL polypropylene
105 bottles. Prior to filtration, 40 mL of KCl (3 M) was added to each sample bottle, and the
106 samples were shaken at 120 rpm for 1 h and then centrifuged at $1600 \times g$ for 10 min (Reigstad
107 et al., 2008). The supernatant was filtered through a syringe filter containing a 0.22 μm
108 filtration membrane; the supernatant was subsequently stored in acid-cleaned 60 mL
109 polypropylene bottles at 4 °C, and analysis was performed after 2 days.

110 In the laboratory, the concentrations of NH_4^+ and NO_3^- in the filtrate were determined by a
111 Nutrient analyzer (Micromac-1000, UK). The NO_3^- ($^{15}NO_3^-$ and $^{14}NO_3^-$) ions of the filtrates
112 were converted to N_2O by denitrifying bacteria (*Pseudomonas aureofaciens*) lacking N_2O
113 reductase activity, and N_2O was quantified by coupled gas chromatography isotope ratio mass
114 spectrometry (GC-IRMS, Thermo Scientific, USA) (Dodsworth et al., 2011a). The ammonia
115 oxidation rates were calculated using the equations of Barraclough, D. (1991) as were the
116 concentrations and N isotope ratios of NO_3^- in the samples incubated for 30 and 120 min,

117 respectively.

118

119 **2.3 DNA extraction and purification**

120 DNA was extracted by the SDS-based extraction method described by [Zhou et al. \(1996\)](#), with
121 some modifications. Briefly, approximately 5 g samples were frozen with liquid nitrogen and
122 milled three times. Then the powdered samples were mixed with 13.5 mL of DNA extraction
123 buffer and 100 μL of proteinase K (10 mg ml^{-1}) in tubes; these tubes were horizontally shaken
124 at 225 rpm for 30 min at 37°C . After shaking, 1.5 mL of 20% SDS was added, and the
125 samples were incubated in a water bath; the temperature of the water bath was maintained at
126 65°C for 2 h. During this period, the tubes were subjected to gentle end-over-end inversions
127 every 15 to 20 min. The supernatant fluids were collected after subjecting the tubes to
128 centrifugation at $6000 \times g$ for 10 min at room temperature; the collected supernatant tubes
129 were subsequently transferred into 50 mL centrifuge tubes. The supernatant fluids were mixed
130 with an equal volume of chloroform: isoamyl alcohol solution (24:1, vol/vol). The aqueous
131 phase was recovered by centrifugation and precipitated with a 0.6 volume of isopropanol at
132 room temperature; this process was carried out for at least 1 h. Crude nucleic acids were
133 obtained by centrifugation at $16,000 \times g$ for 20 min at room temperature; these crude nucleic
134 acids were washed with cold 70% ethanol and resuspended in sterile deionized water; the final
135 volume of this solution was $100 \mu\text{L}$. The crude nucleic acids were purified with a Cycle-Pure
136 Kit (Omega, USA). These crude nucleic acids were then resuspended in the elution buffer, and
137 the final volume of the solution mixture was $50 \mu\text{L}$; this solution was stored at -80°C .

138 **2.4 PCR and clone library construction**

139 16S rRNA gene was amplified with purified genomic DNA as templates using universal
140 primers. The primer pairs A21F ($5'\text{-TTC CGG TTG ATC CYG CCG GA-3}'$) and A958R
141 ($5'\text{-YCC GGC GTT GAM TCC AAT T-3}'$) were chosen for Archaea ([Delong, 1992](#)) and
142 Eubac27F ($5'\text{-AGA GTT TGA TCC TGG CTC AG-3}'$) and Eubac1492R ($5'\text{-GGT TAC CTT}$
143 $\text{GTT ACG ACT T-3}'$) were chosen for bacteria ([Lane, 1991](#)). In a total volume of $50 \mu\text{L}$, the

144 reactions were performed using 1.25 U of Taq DNA polymerase (Takara, Japan). The
145 amplification conditions were as follows: an initial denaturation was carried out at 94 °C for 4
146 min, and then, the same denaturation was continued at 94 °C for 1 min. Thereafter, annealing
147 was carried out at 55 °C for 45 s, while extension was conducted at 72 °C for 60 s; the process
148 was repeated for 30 cycles, followed by a final extension step at 72 °C for 10 min. The PCR
149 products were excised after being separated by gel electrophoresis; a gel-extraction kit
150 (Omega, USA) was used to purify the products in accordance with the manufacturer's
151 instructions. The purified PCR products were cloned into pMD20-T vectors (Takara, Japan)
152 and transformed into competent *Escherichia coli* DH5α cells. To select the positive clones,
153 colony PCR was used to determine the presence of correctly sized inserts containing
154 vector-specific primers M13f (5'-GTA AAA CGA CGG CCA G-3') and M13r (5'-CAG GAA
155 ACA GCT ATG AC-3').

156 **2.5 Sequencing and phylogenetic analysis**

157 All of the clones were sequenced by the dideoxynucleotide chain-termination method. In this
158 procedure, an ABI 3730 capillary electrophoresis sequencer (Applied Biosystem, Inc., USA)
159 was coupled with the T-vector universal primers M13f and M13r. The whole sequence of each
160 clone was spliced using DNAMAN software (version 6.0), and the vector sequences were
161 deleted; the presence of chimeras was checked using the Greengenes chimera check tool
162 (Bellerophon server) ([Huber et al., 2004](#)). The program DOTUR was used to determine the
163 operation taxonomic units (OTU) for each sequence; 97% similarity was considered as the
164 cut-off for the chimeric sequences. To find closely related sequences in the GenBank and
165 EMBL databases for phylogenetic analysis, none of the chimeric sequences were submitted to
166 the Advanced BLAST search program. Phylogenetic trees were constructed using the
167 neighbor-joining method and the software MEGA (version 5.05). A bootstrap analysis was
168 used to provide confidence estimates of the tree topologies.

169 **2.6 Amplification of *amoA* (ammonia monooxygenase subunit A)-related**
170 **sequences.**

171 Archaeal *amoA* gene fragments were amplified using the primer pair Arch-*amoA*AF (5'-STA
172 ATG GTC TGG CTT AGA CG-3') and Arch-*amoA*AR (5'-GCG GCC ATC CAT CTG TAT
173 GT-3') (Francis et al., 2005). Bacterial *amoA* genes were also tested using the bacterial primer
174 sets *amoA* 1F (5'-GGG GTT TCT ACT GGT GGT-3') and *amoA* 2R (5'-CCC CTC KGS AAA
175 GCC TTC TTC-3') (Rotthauwe et al. 1997). PCR cycling was performed by the method of
176 Francis et al. (2005). In this method, PCR products from SS and BS were recovered from the
177 gel slices using a gel-extraction kit (Omega, USA) in accordance with the manufacturer's
178 instructions. The purified PCR products from each type of sample were cloned into the
179 pMD20-T vectors (Takara, Japan) and transformed into competent *Escherichia coli* DH5 α
180 cells. Cloning and sequencing were performed according to the above-mentioned process.
181 Forty to fifty randomly selected colonies per sample were analyzed for the presence of insert
182 archaeal *amoA* gene sequences.

183 **2.7 Quantification of 16S rRNA genes and *amoA* genes**

184 Archaeal and bacterial populations were determined by quantify their 16S rRNA genes with
185 344F-518R (Øvreas et al., 1998) and 518F-786R primer pairs (Muyzer et al., 1993),
186 respectively. In addition, the abundance of AOA and AOB were quantified using
187 amo196F-amo277R (Treich et al., 2005) and amoA-1F and amoA-2R (Rotthauwe et al.,
188 1997) primers, respectively. All sample and standard reactions were performed in triplicate.
189 The SYBR Green I method was used for this analysis. The 20 μ L reaction mixture contained 1
190 μ L of template DNA (10 ng), a 0.15 μ M concentration of each primer, and 10 μ L of Power
191 SYBR Green PCR master mix (Applied Biosystems Inc., USA); this reaction mixture was
192 analyzed with ROX and SYBR Green I. The PCR conditions were as follows: 10 min at 50 °C,
193 2 min at 95 °C; 40 cycles consisting of 15 s at 95 °C and 1 min at 60 °C; 15 s at 95 °C, 1 min
194 at 60 °C, and 15 s at 95 °C to make the melting curve (Wang et al., 2009). Melting curve
195 analysis was performed after amplification, and the cycle threshold was set automatically
196 using system 7500 software v2.0 Patch 6. The efficiencies of the qPCR runs were 87.8-105.6%

197 ($R^2=0.992-0.999$) for 16S rRNA genes and 102% ($R^2=0.998$) for AOA. Primers targeting
198 different genes are listed in Table 1.

199 **2.8 Sample processing for FISH**

200 To visualize Crenarchaea cells *in situ*, FISH was performed according to the procedure
201 described by [Orphan et al. \(2002, 2009\)](#). Small aliquots of sediment were fixed overnight at
202 4 °C using 2 % formaldehyde in 1×PBS [145 mM NaCl, 1.4 mM NaH₂PO₄, 8 mM Na₂HPO₄
203 (pH =7.4)]; these aliquots of sediments were washed twice with 1×PBS and stored at –20 °C
204 in ethanol: PBS (1:1, vol/vol) medium. The total supernatant was filtered through a
205 polycarbonate filter (Millipore) under low vacuum (<5 psi; 1psi=6.89 kPa). Filters were cut
206 into suitably sized pieces and transferred onto untreated, round, 1 in glass slides. The transfer
207 of filters onto glass slides was performed according to the procedure described by [Murray et al.](#)
208 [\(1998\)](#). In this process, 5 µL of a 1×PBS solution was spotted onto a glass slide that was
209 scored with a diamond pen prior to mapping, and half of the freshly prepared filter was used to
210 invert the sample onto the slide; this inverted sample was then air-dried. Prior to FISH, the
211 samples on the glass slides were treated with an EtOH dehydration series (50, 75, and 100%
212 EtOH), dried, and stored at –20 °C. Hybridization and wash buffers were prepared according
213 to the procedure described by [Pernthaler et al., 2001](#). Here, 20 µL of hybridization buffer
214 containing 35% or 20% formamide was added to the samples on the glass slides. FITC-labeled
215 oligonucleotide Cren679 probe described by [Labrenz et al. \(2010\)](#), was added to the
216 hybridization buffer so that the final solution had a concentration of 5 ng µL⁻¹.

217 The hybridization mixtures on the slides were incubated for 1.5 h at 46 °C in a
218 pre-moistened chamber. After hybridization, the slides were transferred into a preheated wash
219 buffer and incubated for an additional 15 min at 48 °C. The samples were rinsed in distilled
220 water and air-dried in the dark. The microscopic images of the hybridized samples were
221 recorded on a Leica Imager (Leica, DMI 4000B, Germany).

222 **2.9 Nucleotide sequence accession numbers**

223 The clone libraries for archaeal communities (21F-958R), bacterial communities (27F-1492R),

224 and archaeal *amoA* genes(*amoAF-amoAR*) were constructed. All of the small-subunit rRNA
225 gene sequences and the *amoA* sequences were deposited in the GenBank/EMBL nucleotide
226 sequence database under the following accession numbers: KP784719 to KP784760 for partial
227 16S rRNA gene sequences and KP994442 to KP994448 for the *amoA* sequences.

228

229 **3 Results**

230 **3.1 Water chemistry**

231 The hot spring water (pH = 7.7) contained Ca (20.25 mg L⁻¹), K (41.97 mg L⁻¹), Mg (3.986 mg
232 L⁻¹), Na (313.3 mg L⁻¹), SiO₂ (130.3 mg L⁻¹), HCO₃⁻ (963 mg L⁻¹), NH₄⁺-N (102.61 μg L⁻¹),
233 NO₃⁻-N (7.68 μg L⁻¹), F⁻ (9.158 mg L⁻¹), Cl⁻ (418.9 mg L⁻¹) and SO₄²⁻ (24.96 mg L⁻¹). The
234 bottom water had a temperature of 77 °C, higher than the surface water that had a temperature
235 of 55 °C. This hot spring was previously categorized as a Na-HCO₃ spring due to the high
236 concentration of alkaline metal ions (K, Na, and Ca) ([Zhang et al., 2008b](#)).

237

238 **3.2 Ammonia oxidation rates**

239 In the surface and bottom sediments (without NH₄⁺ stimulation), the near *in situ* rates of
240 ammonia oxidation were estimated to be 4.80 ± 0.2 and 5.30 ± 0.5 nmol N g⁻¹h⁻¹ using
241 ¹⁵N-NO₃⁻ pool dilution technique, respectively. In the meantime, the nitrate concentration
242 increased from 2.84 ± 2 μM to 3.25 ± 2 μM in the surface sediments and from 2.33 ± 3 μM to
243 2.62 ± 3 μM in the bottom sediments, further providing evidences for strong nitrification
244 activity under *in situ* conditions in the hot springs. Furthermore, the potential activity of
245 ammonia oxidation was determined with ammonium amendments. The nitrate concentration
246 increased significantly upon the addition of NH₄⁺, and the ammonia oxidation rates recorded
247 in the surface sediments and bottom sediments (with NH₄⁺) were 5.70 ± 0.6 and 7.10 ± 0.8
248 nmol N g⁻¹h⁻¹, respectively.

249 **3.3 Archaeal community composition and phylogenetic analysis.**

250 A total of 152 archaeal clone sequences of 16S rRNA genes were obtained in this study.
251 Phylogenetic analysis showed the distribution of the clone sequences into three monophyletic
252 groups: Thaumarchaeota, Crenarchaeota, and Euryarchaeota (Fig 4). In this study, the most
253 abundant archaeal phylum was Thaumarchaeota. Among them, two phylotypes (SS-A19 and
254 BS-A1) were the most dominant archaeal lineage, representing 89% and 86% of the cloned
255 archaeal sequences in surface and bottom sediments, respectively. These sequences were
256 closely related to the thermophilic, autotrophic, ammonia-oxidizing archaeal “*Ca. N.*
257 *yellowstonii*” (de la Tarre et al., 2008). The seven archaeal OTUs found here belonged to
258 Crenarchaeota, which contains sequences recovered from hydrothermal vents and hot spring
259 environments. In addition, two phylotypes (BS-A47 and BS-A8) that were branched with
260 uncultured sequences belonged to *Desulfurococcales*, which was also recovered from
261 sediments of the hot spring. Euryarchaeota also occurred in both the sediments, but with
262 relatively low abundances. Phylotype BS-A80 is associated with *Geoglobus ahangari*, which
263 belongs to *Archaeoglobales* and is capable of oxidizing organic acids (Kashefi, et al., 2002).
264 SS-A12, which represents four clones recovered from the surface sediments, showed 93%
265 similarity to an uncultured archaeal clone that was recovered from the Spring River. SS-A47
266 belonged to the *Thermoplasmatales* that were 96% similar to their nearest neighbor sequence,
267 which were collected from the Spring River. The other euryarchaeotal sequences BS-14 and
268 BS-A80 were similar to their uncultured counterparts (from 96 to 99% identity), which were
269 mostly recovered from high-temperature geothermal environments.

270 **3.4 Community analysis of AOA**

271 A total of 113 archaeal *amoA* gene fragments were obtained from the two samples. They were
272 all branched within the four distinct clusters of archaeal *amoA* sequences: Cluster
273 *Nitrosopumilus*, *Nitrososphaera*, *Nitrosotalea*, *Nitrosocaldus* (Fig 5). *Nitrosopumilus* Cluster
274 contained phylotypes SS-AOA-4 and BS-AOA-22, which branched with large numbers of
275 sequences recovered from the sediments and water samples in the marine or fresh
276 environments. The other clade, Cluster *Nitrososphaera*, has two phylotypes representing 44

277 sequences. OTU BS-AOA-62 contained 18 sequences, which was closely related to sequences
278 from soil. The clone SS-AOA-76 clustered within clade *Nitrososphaera* and showed up to 99%
279 sequence identity to an uncultured archaeon clone GHL2_S_AOA_19 (JX488447) obtained
280 from lake sediment.

281 Cluster *Nitrosotalea* had 1 phylotype (SS-AOA-65) with 11 sequences (12% of the total
282 sequences). The closely related sequences in this cluster included characteristic crenarchaeotal
283 group sequences that were obtained from alpine soil (with 98% identity). Another clone,
284 MX_3_OCT_18 (DQ501052), from estuary sediment was 96% similar.

285 Cluster *Nitrosocaldus* contained two phlotypes (BS-AOA-15 and SS-AOA-50) with 34
286 sequences (30% of the total sequences). They were closely related to the geothermal water
287 sequences, with 95-99% similarity. Furthermore, Cluster *Nitrosocaldus* mainly represented
288 previously described ThAOA/HWCG III (Prosser and Nicol, 2008). Notably, the recently
289 reported *amoA* gene sequence of “*Ca. N. yellowstonii*” (EU239961) (De la Torre et al., 2008)
290 showed 85% sequence identity to clones BS-AOA-15 and SS-AOA-50.

291 3.5 Quantitative PCR

292 The qPCR results (Fig. 2b) indicated that the abundance of the archaeal 16S rRNA gene in the
293 two samples was similar, ranging from 1.28 to 1.96×10^7 gene copies g^{-1} of dry weight of
294 sediments. However, the abundance of the bacterial 16S rRNA gene varied greatly, ranging
295 from 6.86×10^6 to 4.25×10^8 gene copies g^{-1} of dry weight of sediments (Fig. S2 in the
296 Supplement). The copy numbers of archaeal *amoA* genes in the surface and bottom sediments
297 are 2.75×10^5 and 9.80×10^5 gene copies g^{-1} sediment, respectively. The copy numbers of the
298 archaeal 16S rRNA genes in the bottom sediments were significantly higher than those of the
299 bacterial 16S rRNA genes, with a ratio of 28.57. However, in surface sediments, the ratio of
300 bacterial 16S rRNA genes to archaeal 16S rRNA genes is 3.32.

301 3.6 FISH

302 FISH was used to analyze the relative abundance of Crenarchaea in two samples. As expected,
303 most metabolically active Crenarchaea cells and aggregated cells were detected by FISH

304 probes (Cren679) (Fig 3). Based on the qPCR results, a high abundance of crenarchaea in the
305 hot spring sediments harbored *amoA* genes, providing strong evidence supporting the
306 important role of Crenarchaea in the oxidation of ammonia.

307

308 **4 Discussion**

309 **4.1 Environmental factors affecting the occurrence of ammonia-oxidizing** 310 **microorganisms**

311 Temperature is likely a very important factor influencing microbial community structure. This
312 interpretation is supported by the results of qPCR (Fig. 2b and Fig. S2). The sediment samples
313 from the bottom of pool (T=77 °C) are dominated by Archaea, whereas the sediment samples
314 from the margin of pool (T=55 °C) are dominated by Bacteria. In addition, no AOB were
315 detected in both bottom and margin samples, indicating that it might be difficult for AOB to
316 inhabit in high-temperature hot spring environments (Lebedeva et al., 2005; Hatzenpichler et
317 al., 2008). Additionally, the abundance of AOA *amoA* gene in bottom sediments is slightly
318 higher than that in margin sediments, reflecting that although AOA can adapt to a wide range
319 of temperature, higher temperature could be more favorable to the growth of AOA (de la Torre,
320 et al., 2008; Hatzenpichler et al., 2008; Jiang et al., 2010).

321 Ammonia concentration may be another factor that influences the potential activity of AOA
322 and AOB in hot springs. Because AMO in AOA has a much higher affinity for the substrate
323 compared to a similar process in AOB, the ability of AOA to compete for ammonia in
324 oligotrophic hot spring environments is also substantially higher than that of AOB
325 (Hatzenpichler et al., 2008). In Gongxiaoshe hot spring, the ammonia concentration of 102.61
326 $\mu\text{g L}^{-1}$ is lower compared to other hot springs with high ammonia concentrations. This
327 relatively low ammonia concentration may possibly be responsible for the absence of AOB in
328 Gongxiaoshe hot spring.

329 **4.2 Composition and abundance of AOA**

330 The rarefaction curves (Fig. S3) for archaeal 16S rRNA genes and *amoA* genes in the surface
331 and bottom sediment samples reached a plateau, and their coverage values were relatively
332 high (89-99%). This result indicated that a large part of the archaeal/*amoA* diversity at this

333 spring was probably included in the archaeal/*amoA* clone libraries. The majority of archaeal
334 sequences were closely related to ‘*Ca. N. yellowstonii*’, a known AOA, which may be
335 responsible for the oxidation of ammonia in this spring.

336 In this study, phylogenetic analyses of archaea *amoA* genes showed that *Candidatus*
337 *Nitrosocaldus yellowstonii* dominated in both of the samples. This result also agreed with
338 previous hot spring observations reported by [Dodsworth et al. \(2011b\)](#) and [Hou et al. \(2013\)](#).
339 According to the sequences retrieved from NCBI, *Nitrosotalea* and *Nitrososphaera* clusters
340 were closely related to the cluster soil. One possibility is that some of the *amoA* genes
341 obtained in this study may derive from soil AOA, particularly those sequences in cluster
342 *Nitrosotalea* and cluster *Nitrososphaera*, which have been widely found in sediments and soils.
343 Those AOA from soil might have evolved multiple times and have adapted to
344 high-temperature environments. Based on the analysis of the real-time PCR and FISH
345 methods, our data indicate that the abundance of AOA is relatively high in both samples. The
346 archaeal *amoA* gene copy numbers ranged from 2.75 to 9.80×10^5 per gram dry weight of
347 sediments in this study. This is comparable to the abundance in other hot water springs
348 [10^4 - 10^5 copies g^{-1} ([Dodsworth et al., 2011b](#))], but is lower than the abundance of the archaeal
349 *amoA* gene in non-thermal environments, such as paddy rhizosphere soil [10^6 - 10^7 copies g^{-1}
350 ([Chen et al., 2008](#))] and marine sediments [10^7 - 10^8 copies g^{-1} ([Park et al., 2008](#))]. The bacterial
351 *amoA* genes were not detected, indicating that AOB is absent or is a minority in this hot spring
352 ecosystem. A predominance of archaeal *amoA* genes versus bacterial *amoA* genes indicated
353 that ammonia oxidation may be due to the activity of archaea in the Gongxiaoshe hot spring.

354 **4.3 The role of AOA in the nitrification of terrestrial geothermal environments**

355 In the surface and bottom sediments (without NH_4^+), the ammonia oxidation rates calculated
356 from the ^{15}N - NO_3^- pool dilution data were 4.80 ± 0.2 and 5.30 ± 0.5 $nmol\ N\ g^{-1}h^{-1}$,
357 respectively. The ammonia oxidation rates recorded in the surface sediments and bottom
358 sediments (with NH_4^+) were 5.70 ± 0.6 and 7.10 ± 0.8 $nmol\ N\ g^{-1}h^{-1}$, respectively. Moreover,
359 the rates reported here were comparable with those observed in the two US Great Basin (GB)
360 hot springs [5.50 - 8.60 $nmol\ N\ g^{-1}h^{-1}$ ([Dodsworth et al., 2011b](#))] and in two acidic (pH = 3, T =
361 85 °C) Iceland hot springs [2.80 - 7.00 $nmol\ NO_3^-\ g^{-1}h^{-1}$ ([Reigstad et al., 2008](#))]. However, the

362 rates reported in this study were lower than those observed in some wetland sediments and
363 agricultural soils [85-180 nmol N g⁻¹h⁻¹ (White and Reddy, 2003; Booth et al., 2005)].

364 The ammonia oxidation rates in bottom sediments (without NH₄⁺) were slightly higher than
365 those observed in surface sediments (without NH₄⁺). This result agrees with the distribution of
366 archaeal *amoA* genes, which were found to be in higher abundance in the bottom sediment
367 than in the surface sediment. High abundance of ammonia-oxidizing archaea corresponds to
368 high ammonia oxidation rates, which were consistent with the results reported by Isobe et al.
369 (2012). Compared with the incubation experiments unamended with NH₄⁺, the ammonia
370 oxidation rate appeared to be stimulated after amendment with NH₄⁺ (1 M). There are
371 indications that the ammonia concentration is an important factor affecting the rates of
372 nitrification (Hatzenpichler et al., 2008).

373 To understand the relationship between the ammonia oxidation rates and abundances of
374 *amoA* in the two samples, we specifically estimated the contribution of archaeal cells to
375 nitrification. By assuming two *amoA* copies per cell (Bernander and Poplawski, 1997) and by
376 comparing the ammonia oxidation rates with the qPCR results of AOA *amoA* per gram
377 (however, some uncertainties of this method may still exist, with respect to the stage of cell
378 cycle and the diversity of archaea), the cell-specific nitrification rates were estimated to be
379 0.410 fmol N cell⁻¹h⁻¹ and 0.790 fmol N cell⁻¹h⁻¹ in the surface and bottom sediments of the
380 hot spring, respectively. These results are much higher than those for AOA in US hot springs
381 [0.008-0.01 fmol N cell⁻¹h⁻¹ (Dodsworth et al., 2011b)]. It is interesting that although the GBS
382 hot spring possesses higher *amoA* gene copies (3.50-3.90 × 10⁸ gene copies g⁻¹ of dry weight)
383 and higher NH₄⁺ concentration (663 μg L⁻¹), it exhibits a lower cell-specific nitrification rate
384 than Gongxiaoshe hot spring. This may imply that both the abundance of AOA and the NH₄⁺
385 concentration are not important factors that control the cell-specific nitrification rates in
386 high-temperature hot spring environments. The difference in cell-specific nitrification rates
387 between the Gongxiaoshe hot spring and the GBS hot spring may reflect the difference of
388 AOA population structure in those two hot springs (Gubry-Rangin et al., 2011; Pester et al.,
389 2012). In line with this AOA heterogeneity, cell-specific nitrification rates do not reflect the
390 overall AOA abundance or NH₄⁺ concentration in these AOA-dominated hot springs. Alves et
391 al. (2013) reported a similar case where soil dominated by AOA (clade A) exhibited the lowest

392 nitrification rates, in spite of harboring the largest AOA populations. These results also suggest
393 the importance of cultivation studies for comparative analysis of environmentally
394 representative AOA in a wide variety of hot springs.

395

396 **5 Conclusions**

397 Combination of $^{15}\text{N-NO}_3^-$ pool dilution and molecular analyses demonstrate that the
398 oxidation of ammonia by AOA occurs actively in the high-temperature Gongxiaoshe
399 geothermal system. The presence of considerable *in situ* nitrification rates in the hot spring
400 is likely due to two dominant groups that include phylotypes that are closely related to the
401 autotrophic AOA '*Ca. N. yellowstonii*'. The detection of archaeal *amoA* genes and the
402 absence of AOB indicate that archaeal ammonia oxidizers, rather than AOB, significantly
403 contribute to the nitrification in the Gongxiaoshe geothermal systems. Due to the AOA
404 heterogeneity, cell-specific nitrification rates may not reflect the overall AOA abundance or
405 NH_4^+ concentration in the AOA-dominated hot springs. Our results shed light on the
406 importance of AOA in driving the oxidation of ammonia in high-temperature environments,
407 which may be ubiquitous in other terrestrial hot springs on Earth.

408

409

410

411

412 **References**

413 Alves RJ, Wanek W, Zappe A, Richter A, Svenning MM, Schleper C and Urich T.:
414 Nitrification rates in Arctic soils are associated with functionally distinct populations of
415 ammonia-oxidizing archaea. *ISME J* 7: 1620-1631, 2013.

416 Appelo, C.A.J and Postma, D.: *Geochemistry, groundwater, and pollution*. Balkema,
417 Rotterdam, 1996.

418 Beman J M, Popp BN and Francis C A.: Molecular and biogeochemical evidence for ammonia
419 oxidation by marine crenarchaeota in the Gulf of California. *ISME J* 2: 429-441, 2008.

420 Barraclough. D.: The use of mean pool abundances to interpret ^{15}N tracer experiments. *Plant*

421 and Soil, 131, 89-96, 1991.

422 Bernander, R., and Poplawski.: A. Cell cycle characteristics of thermophilic archaea. J
423 Bacteriol. 179: 4963-4969, 1997.

424 Booth, M. S., Stark, J. M., and Rastetter, E.: Controls on nitrogen cycling in terrestrial
425 ecosystems: a synthetic analysis of literature data. Ecol Monogr 75: 139-157, 2005.

426 Chen X P, Zhu Y G, Xia Y, Shen J P and He J Z.: Ammonia oxidizing archaea: important
427 players in paddy rhizosphere soil? Environ Microbiol. 10: 1978-1987, 2008.

428 De la Torre, J., C.Walker, A. Ingalls, M. Koenneke, and D. Stahl.: Cultivation of a
429 thermophilic ammonia oxidizing archaeon synthesizing crenarchaeol. Environ Microbiol, 10,
430 810-818, 2008.

431 Delong, E. F.: Archaea in coastal marine environments. Proc. Natl. Acad. Sci. USA, 89:
432 5685-5689, 1992.

433 Dodsworth, J.A., Hungate, B., Torre, J., Jiang, H., and Hedlund, B. P.: Measuring nitrification,
434 denitrification, and related biomarkers in continental geothermal ecosystems. Methods
435 Enzymol, 486: 171-203, 2011a.

436 Dodsworth J A, Hungate B A, Hedlund B P.: Ammonia oxidation, denitrification and
437 dissimilatory nitrate reduction to ammonium in two US Great Basin hot springs with abundant
438 ammonia-oxidizing archaea. Environ Microbiol.13: 2371-2386, 2011b.

439 Francis C A, Robert s K J, Beman J M, Santoro A E and Oakley B B.: Ubiquity and diversity
440 of ammonia-oxidizing archaea in water columns and sediments of the ocean. Proc. Natl. Acad.
441 Sci. U.S.A, 102(41): 14683-14688, 2005.

442 Francis, C A, Beman, J and Kuypers, M.: New processes and players in the nitrogen cycle: the
443 microbial ecology of anaerobic and archaeal ammonia oxidation. Appl Environ Microbiol. 1:
444 19-27, 2007.

445 Gerbl, F W, Weidler, G W, Wanek, W, Erhardt, A and Stan-Lotter H.: Thaumarchaeal
446 ammonium oxidation and evidence for a nitrogen cycle in a subsurface radioactive thermal
447 spring in the Austrian Central Alps. Frontiers in Microbiology. doi: 10.3389/fmicb. 2014.
448 00225, 2014.

449 Gubry-Rangin C, Hai B, Quince C, Engel M, Thomson B C, James P, Schloter M, Griffiths R I,
450 Prosser J I and Nicol G W.: Niche specialization of terrestrial archaeal ammonia oxidizers.

451 Proc Natl Acad Sci USA 108: 21206-21211, 2011.

452 Hatzenpichler, R., E. Lebedeva, E. Spieck, K. Stoecker, A. Richter, H. Daims, and M. Wagner.:
453 A moderately thermophilic ammonia-oxidizing crenarchaeote from a hot spring. Proc. Natl.
454 Acad. Sci. U.S.A. 105, 2134-2139, 2008.

455 He, J., Shen, J., Zhang, L., Zhu, Y., Zheng, Y., Xu, M., and Di, H.: Quantitative analyses of the
456 abundance and composition of ammonia-oxidizing bacteria and ammonia-oxidizing archaea of
457 a Chinese upland red soil under long-term fertilization practices. Environ Microbiol 9,
458 2364-2374, 2007.

459 Hou, W. G., Wang, S., Dong, H. L., Jiang, H. C., Briggs, B. R., Peacock, J. P., Huang, Q. Y.,
460 Huang, L. Q., Wu, G., Zhi, X. Y., Li, W. J., Dodsworth, J. A., Hedlund, B. P., Zhang, C. L.,
461 Hartnett, H. E., Dijkstra, P., and Hungate, B. A.: A Comprehensive Census of Microbial
462 Diversity in Hot Springs of Tengchong, Yunnan Province China Using 16S rRNA Gene
463 Pyrosequencing. PLoS ONE 8(1): e53350. doi:10.1371/journal.pone.0053350, 2013.

464 Huber T, Faulkner G, Hugenholtz P.: Bellerophon: a program to detect chimeric sequences in
465 multiple sequence alignments. Bioinformatics, 20: 2317-2319, 2004.

466 Isobe, K, Koba K, Suwa Y, Ikutani J, Fang Y T, Yoh M, Mo, J. M., Otsuka, S., and Senoo, K.:
467 High abundance of ammonia-oxidizing archaea in acidified subtropical forest soils in southern
468 China after long-term N deposition. FEMS Microbiol. Ecol. 80, 193-203, 2012.

469 Jia, Z. J and Conrad, R.: Bacteria rather than Archaea dominate microbial ammonia oxidation
470 in an agricultural soil. Environ. Microbiol. 11, 1658-1671, 2009.

471 Jiang H C, Huang Q Y, Dong H L, Wang P, Wang F P, Li, W. J., and Zhang, C. L.: RNA-based
472 investigation of ammonia oxidizing archaea in hot springs of Yunnan Province, China. Appl.
473 Environ. Microbiol. 76: 4538-4541, 2010

474 Kashefi, K, Tor, J M, Holmes, D E, Gaw Van Praagh, C.V, Reysenbach, A.L., and Lovley,
475 D.R.: *Geoglobus ahangari* gen. nov., sp. nov., a novel hyperthermophilic archaeon capable
476 of oxidizing organic acids and growing autotrophically on hydrogen with Fe(III) serving as the
477 sole electron acceptor. Int. J. Syst. Evol. Microbiol. 52: 719-728, 2002.

478 Konneke, M., A. E. Bernhard, J. R. de la Torre, C. B. Walker, J. B. Waterbury, and D. A. Stahl.:
479 Isolation of an autotrophic ammonia-oxidizing marine archaeon. Nature, 437: 543-546, 2005.

480 Labrenz M, Sintes E, Toetzke F, Zumsteg A, Herndl G, Seidler M and Jurgens K.: Relevance

481 of a crenarchaeotal subcluster related to *Candidatus Nitrosopumilus maritimus* to ammonia
482 oxidation in the suboxic zone of the central Baltic Sea. *ISME J.* 4, 1496-1508, 2010.

483 Lane, D. J.: 16S/23S rRNA sequencing, p. 115-175. In E. Stackebrandt and M. Goodfellow
484 (eds.), *Nucleic acid techniques in bacterial systematics*. Wiley, Chichester, UK, 1991.

485 Lebedeva E V, Alawi M, Fiencke C, Namsaraev B, Bock E, Spieck E.: Moderately
486 thermophilic nitrifying bacteria from a hot spring of the Baikal rift zone. *FEMS Microbiol*
487 *Ecol*, 54: 297-306, 2005.

488 Li, H. Z, Yang, Q. H, Li, Jian, Gao, H, Li, P and Zhou, H.: The impact of temperature on
489 microbial diversity and AOA activity in the Tengchong Geothermal Field, China. *Scientific*
490 *Reports*, 5: 17056, DOI: 10. 1038/ srep17056. 2015.

491 Murray, A. E., Preston, C. M., Massana, R., Taylor, L. T., Blakis, A., Wu, K and DeLong, E. F.:
492 Seasonal and Spatial Variability of Bacterial and Archaeal Assemblages in the Coastal Waters
493 near Anvers Island, Antarctica, *Appl. Environ. Microbiol.* 64, 2585-2595, 1998.

494 Muyzer, G, E.C. de Waal, and A.G. Uitterlinden.: Profiling of complex microbial populations
495 by denaturing gradient gel electrophoresis analysis of polymerase chain reaction-amplified
496 genes coding for 16S rRNA. *Appl. Environ. Microbiol.* 59, 695-700, 1993.

497 Nicol, G. W., and C. Schleper.: Ammonia-oxidising Crenarchaeota: important players in the
498 nitrogen cycle? *Trends Microbiol.* 14: 207-212, 2006.

499 Nishizawa, M., Koba, K., Makabe, A., Yoshida, N., Kaneko, M., Hirao, S., Ishibashi, J. I.,
500 Yamanaka, T., Shibuya, T., Kikuchi, T., Hirai, M., Miyazaki, J., Nunoura, T., and Takai, K.:
501 Nitrification-driven forms of nitrogen metabolism in microbial mat communities thriving
502 along an ammonium-enriched subsurface geothermal stream. *Geochim Cosmochim Acta* 113:
503 152-173, 2013.

504 Orphan, V J, Turk K A, Green, A M and House, C H.: Patterns of ¹⁵N assimilation and growth
505 of methanotrophic ANME-2 archaea and sulfate-reducing bacteria within structured
506 syntrophic consortia revealed by FISH-SIMS. *Environmental Microbiology*, 11(7), 1777-1791,
507 2009.

508 Orphan, V J, House, C H, Hinrichs, K U, McKeegan, K D and DeLong, E.F.: Multiple
509 archaeal groups mediate methane oxidation in anoxic cold seep sediments. *Proc Natl Acad Sci*
510 *USA*, 99: 7663-7668, 2002.

511 Øvreas, L., S. Jensen, F. L. Daae, and V. Torsvik.: Microbial community changes in a
512 perturbed agricultural soil investigated by molecular and physiological approaches. *Appl.*
513 *Environ. Microbiol.* 64: 2739-2742, 1998.

514 Park S J, Park B J and Rhee S K.: Comparative analysis of archaeal 16S rRNA and amoA
515 genes to estimate the abundance and diversity of ammonia-oxidizing archaea in marine
516 sediments. *Extremophiles*, 12: 605-615, 2008.

517 Pearson, A., Y. Pi, W. Zhao, W. Li, Y.-L. Li, W. Inskeep, Perevalova, A., Romanek, C., Li, S.
518 G., and Zhang, C. L.: Factors controlling the distribution of archaeal tetraethers in terrestrial
519 hot springs. *Appl. Environ. Microbiol.* 74: 3523-3532, 2008.

520 Pernthaler J, Glockner F O, Schonhuber W, Amann R.: Fluorescence in situ hybridization with
521 rRNA-targeted oligonucleotide probes. In: Paul JH (eds) *Methods in microbiology: Marine*
522 *microbiology* Academic Press, San diego, San Francisco, New York, Boston London, Sydney,
523 Tokyo, 207-226, 2001.

524 Pester M, Rattei T, Flechl S, Grongroft A, Richter A, Overmann J, Reinhold-Hurek B, Loy A
525 and Wagner M.: amoA-based consensus phylogeny of ammonia-oxidizing archaea and deep
526 sequencing of amoA genes from soils of four different geographic regions. *Environ Microbiol*,
527 14: 525-539, 2012.

528 Prosser J I & Nicol G W.: Relative contributions of archaea and bacteria to aerobic ammonia
529 oxidation in the environment. *Environ Microbiol* 10: 2931-2941, 2008.

530 Reigstad, L., A. Richter, H. Daims, T. Urich, L. Schwark, and C. Schleper.: Nitrification in
531 terrestrial hot springs of Iceland and Kamchatka. *FEMS Microbiol Ecol* 64, 167-174, 2008.

532 Rotthauwe J H, Witzel K P, Liesack W.: The ammonia monooxygenase structural gene amoA
533 as a functional marker: molecular fine-scale analysis of natural ammonia-oxidizing
534 populations. *Appl Environ Microbiol*, 63: 4704-4712, 1997.

535 Shock, E. L., Holland. M, Meyer-Dombard, D. R., and J. P. Amend.: Geochemical sources of
536 energy for microbial metabolism in hydrothermal ecosystems: Obsidian Pool, Yellowstone
537 National Park, USA, In W. P. Inskeep and T. R. McDermott (ed.), *Geothermal biology and*
538 *geochemistry in Yellowstone National Park*, vol. 1, p. 95-112, 2005.

539 Spear, J R, Barton, H A, Robertson, C E, Francis, C A and Pace, N R.: Microbial Community
540 Biofabrics in a Geothermal Mine Adit. *Appl Environ Microbiol*, 73(9): 6172-6180, 2007.

541 Treusch, A., S. Leininger, A. Kletzin, S. Schuster, H. Klenk, and C. Schleper.: Novel genes for
542 nitrite reductase and Amo-related proteins indicate a role of uncultivated mesophilic
543 crenarchaeota in nitrogen cycling. *Environ Microbiol.* 7, 1985-1995, 2005.

544 Vitousek, P. M., J. Aber, R. W. Howarth, G. E. Likens, P. A. Matson, D. W. Schindler, W. H.
545 Schlesinger, and G. D. Tilman.: Human alteration of the global nitrogen cycle: Causes and
546 consequences. *Ecological Applications* 7: 737-750, 1997.

547 Wang S, Xiao X, Jiang L, Peng X, Zhou H, Meng J, Wang F.: Diversity and abundance of
548 ammonia-oxidizing Archaea in hydrothermal vent chimneys of the Juan de Fuca Ridge. *Appl*
549 *Environ Microbiol*, 75: 4216-4220, 2009.

550 Weidler, G. W., M. Dornmayr-Pfaffenhuemer, F. W. Gerbl, W. Heinen, and H. Stan-Lotter.:
551 Communities of Archaea and Bacteria in a subsurface radioactive thermal spring in the
552 Austrian Central Alps, and evidence of ammonia-oxidizing Crenarchaeota. *Appl. Environ.*
553 *Microbiol.* 73: 259-270, 2007.

554 White, J R, and Reddy, K R.: Potential nitrification and denitrification rates in a
555 phosphorous-impacted subtropical peatland. *J Environ Qual.* 32: 2436-2443, 2003.

556 Wuchter, C., Abbas, B., Coolen, M. J. L., Herfort, L., van Bleijswijk, J., Timmers, P., Strous,
557 M., Teira, V., Herndl, G. J., Middelburg, J. J., Schouten, S., and Damste, J. S. S.: Archaeal
558 nitrification in the ocean, *P. Natl. Acad. Sci. USA*, 33, 12317-12322, 2006.

559 Xie, W., Zhang, C. L., Wang, J., Chen, Y., Zhu, Y., Torre, J. R., Dong, H., Hartnett, H.E.,
560 Hedlund, B.P., Klotz, M.G.: Distribution of ether lipids and composition of the archaeal
561 community in terrestrial geothermal springs: impact of environmental variables.
562 *Environmental Microbiology.* <http://dx.doi.org/10.1111/1462-2920.12595>, 2014.

563 Zhang, C. L., Ye, Q., Huang, Z., Li, W., Chen, J., Song, Z., Zhao, W., Bagwell, C., Inskeep, W.
564 P., Ross, C., Gao, L., Wiegel, J., Romanek, C. S., Shock, E. L., and Hedlund, B. P.: Global
565 occurrence of archaeal amoA genes in terrestrial hot springs, *Appl. Environ. Microb.*, 74,
566 6417-6426, 2008a.

567 Zhang G, Liu C Q, Liu H, Jin Z, Han G, and Li, L.: Geochemistry of the Rehai and Ruidian
568 geothermal waters, Yunnan Province, China. *Geothermics*, 37: 73-83, 2008b.

569 Zhou, J., M. Bruns, and J. Tiedje.: DNA recovery from soils of diverse composition, *Appl.*
570 *Environ. Microbiol*, 62, 316-322, 1996.

571

572 **Table 1.** FISH probe and PCR primer pairs used in this study

Application	Probe/ Primer set	Specificity	sequence(5'-3')	FA(%)/ AT(°C) ^a	Reference
FISH	Cren679	Crenarchaeota	TTTTACCCCTTCCTCCG	35	Labrenz M, et al. 2010
qPCR	518F	Bacteria	CCAGCAGCCGCGTAAT	57	Muyzer et al. 1993
	786R		GATTAGATACCCTGGTAG		
	344F	Archaea	ACGGGGCGCAGCAGGCGGA	60	Øvreas et al., 1998
	518R		ATTACCGCGGCTGCTGG		
	<i>amo</i> 196F	Archaeal	GGWGTKCCRGRACWGCMAC	60	Treusch et al., 2005
	<i>amo</i> 277R	<i>amoA</i>	CRATGAAGTCRTAHGGRTADCC		
Clone library	A21F	Archaea	TTCCGGTTGATCCYGCCGGA	55	DeLong, 1992
	A958R		YCCGGCGTTGAMTCCAATT		
	Eubac27F	Bacteria	AGAGTTTGATCCTGGCTCAG	55	Lane, 1991
	Eubac1492R		GGTTACCTTGTTACGACTT		
	Arch- <i>amo</i> AF	Archaeal	STAATGGTCTGGCTTAGACG	53	Francis et al., 2005
	Arch- <i>amo</i> AR	<i>amoA</i>	GCGGCCATCCATCTGTATGT		
	<i>amoA</i> 1F	Bacterial	GGGGTTTCTACTGGTGGT	60	Rotthauwe et al. 1997
	<i>amoA</i> 2R	<i>amoA</i>	CCCCTCKGSAAAGCCTTCTTC		

573 ^aFA, Formamide; AT, Annealing Temperature

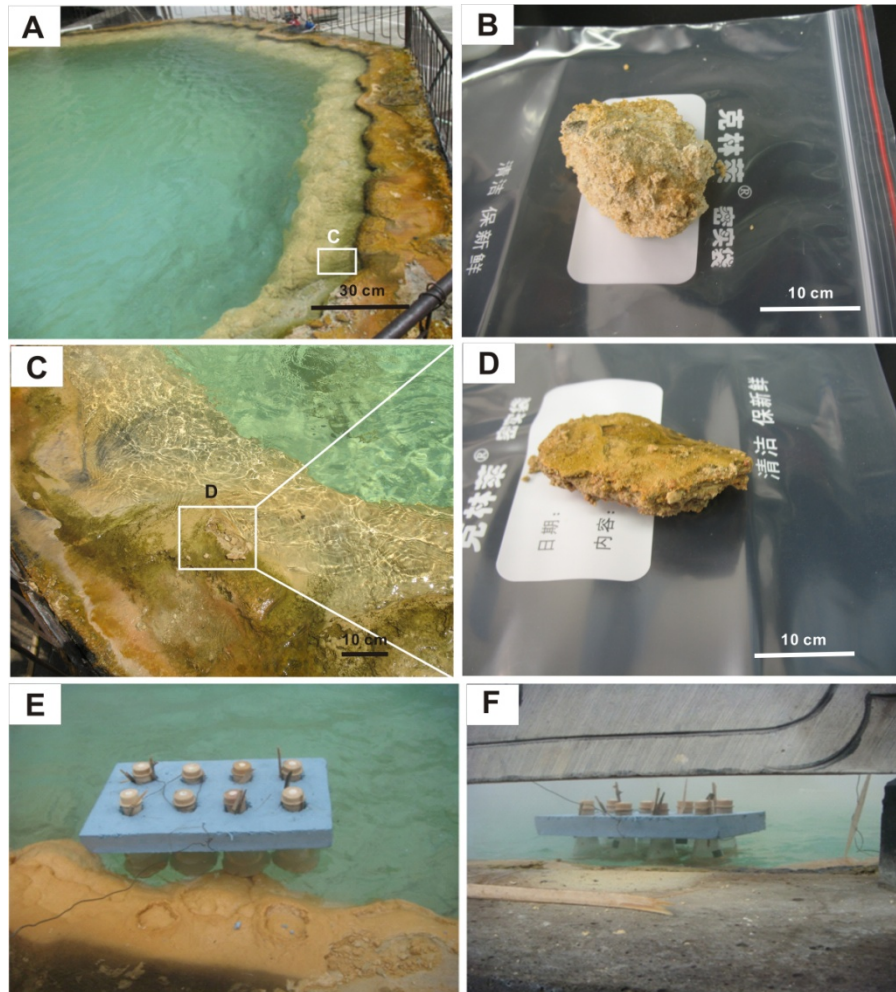
574

575

576

577

578



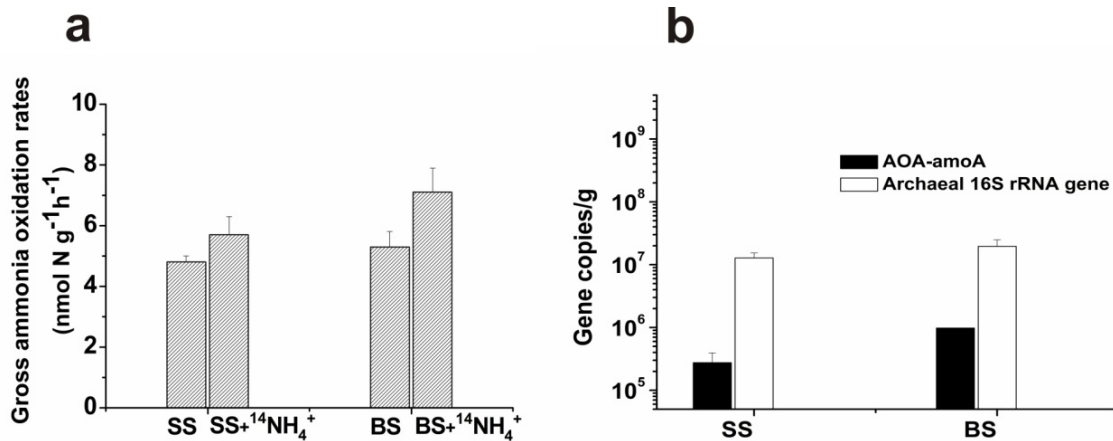
579

580 **Figure 1.** The Gongxiaoshe hot spring, located in the Ruidian geothermal area. (a). A full
 581 view of the spring; (b). Bottom sediments of the hot spring, designated as BS; (c). An enlarged
 582 view of the white box from Fig 1a, surface sediments of the hot spring; (d). Surface sediments
 583 of the hot spring designated as SS; and (e, f), *In situ* nitrification activity and potential
 584 nitrification activity experiments in the field.

585

586

587



588

589 **Figure 2.** (a) Gross ammonia oxidation rates calculated from ¹⁵N-NO₃⁻ pool dilution
 590 experiments on amended (add ¹⁴NH₄⁺) or unamended SS and BS sediment slurries. It defines
 591 that the amendment with “¹⁵NO₃⁻” represents *in situ* nitrification activity, while ¹⁵NO₃⁻ plus
 592 ¹⁴NH₄⁺ is considered as potential nitrification activity. Bars represent the mean and standard
 593 error of the mean (n = 3) for 30 and 120 min incubation. (b) Abundance of archaeal 16S rRNA
 594 genes and archaeal amoA genes for SS and BS samples collected from Gongxiaohe hot
 595 spring. Data are expressed as gene copies per gram of sediment (dry weight). Error bars
 596 represent the standard deviation of the mean (n=3).

597

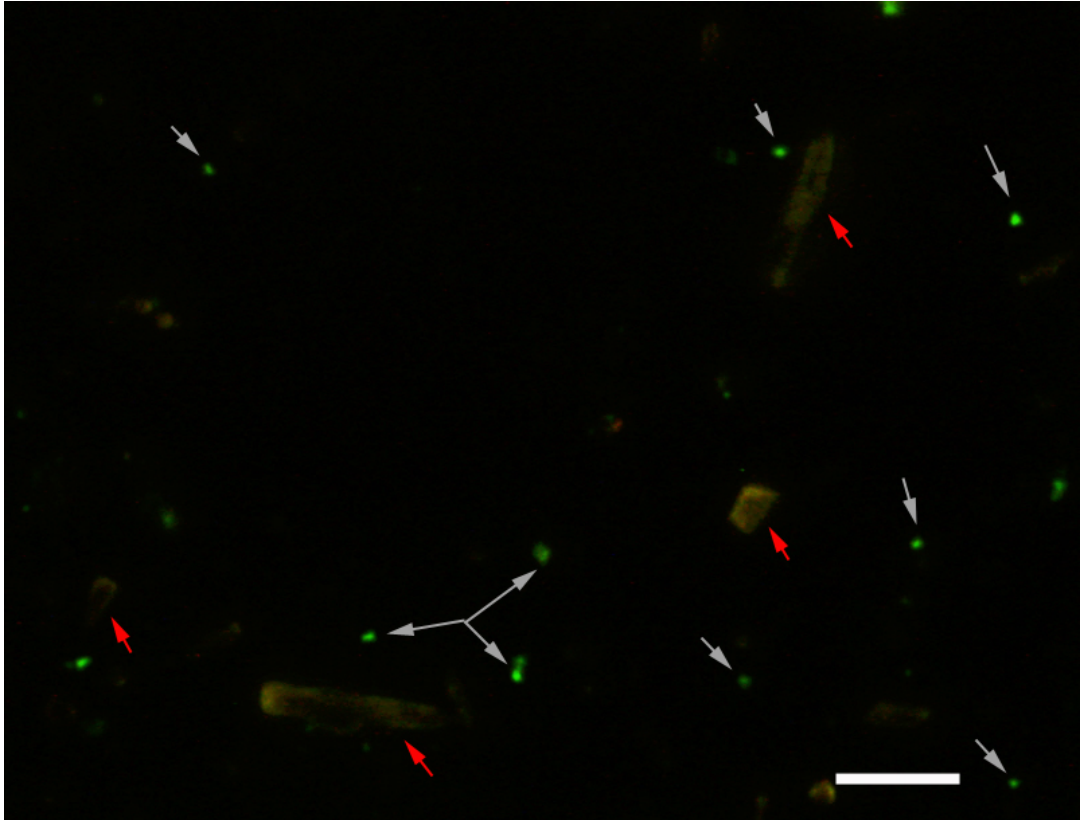
598

599

600

601

602



603

604 **Figure 3.** Epifluorescence photomicrograph of Crenarchaeota cells and cell aggregates. (White
605 and red arrows show the cells and carbonate crystals, respectively. Scale bar corresponds to 20
606 μm)

607

608

609

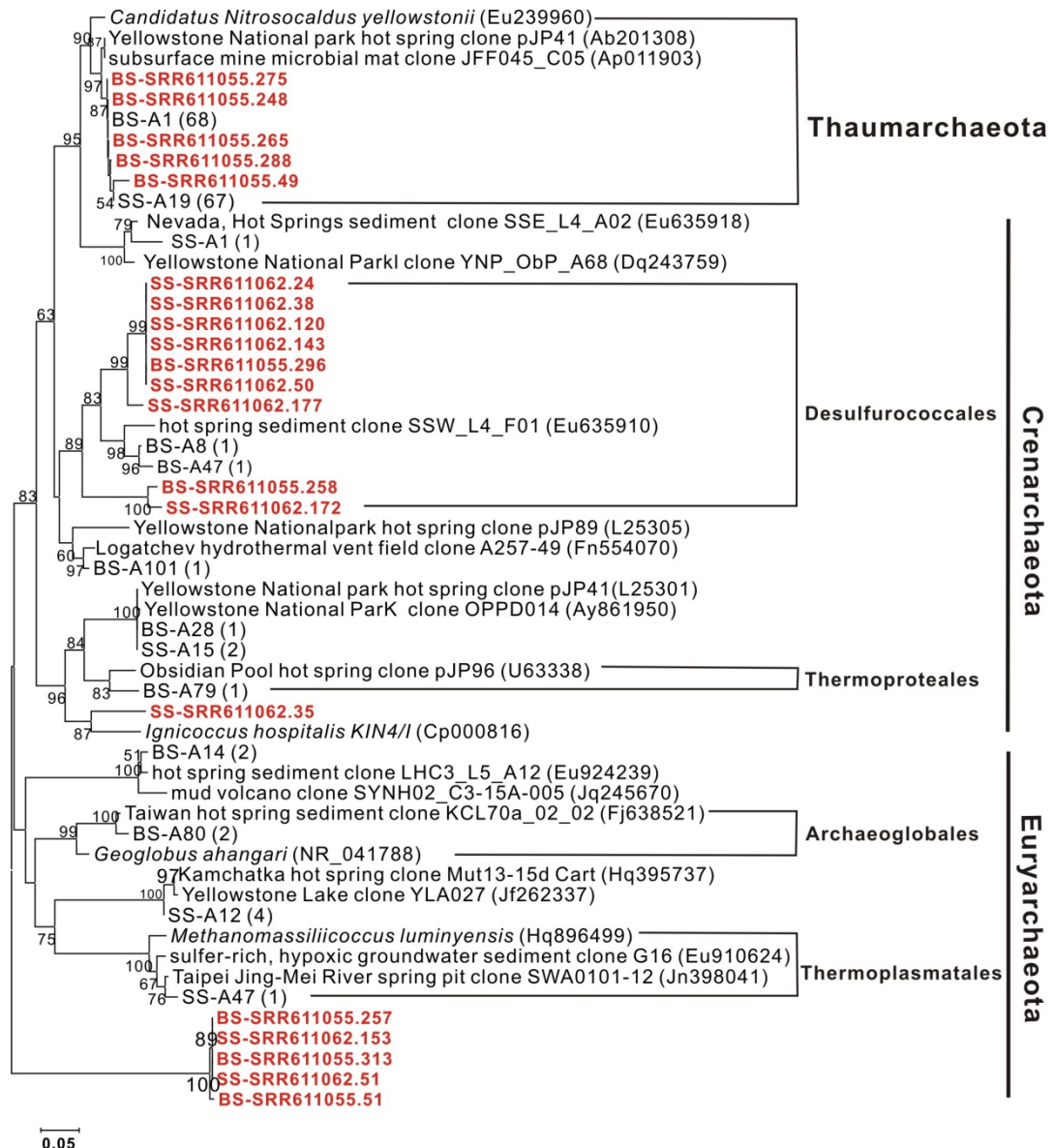
610

611

612

613

614



615

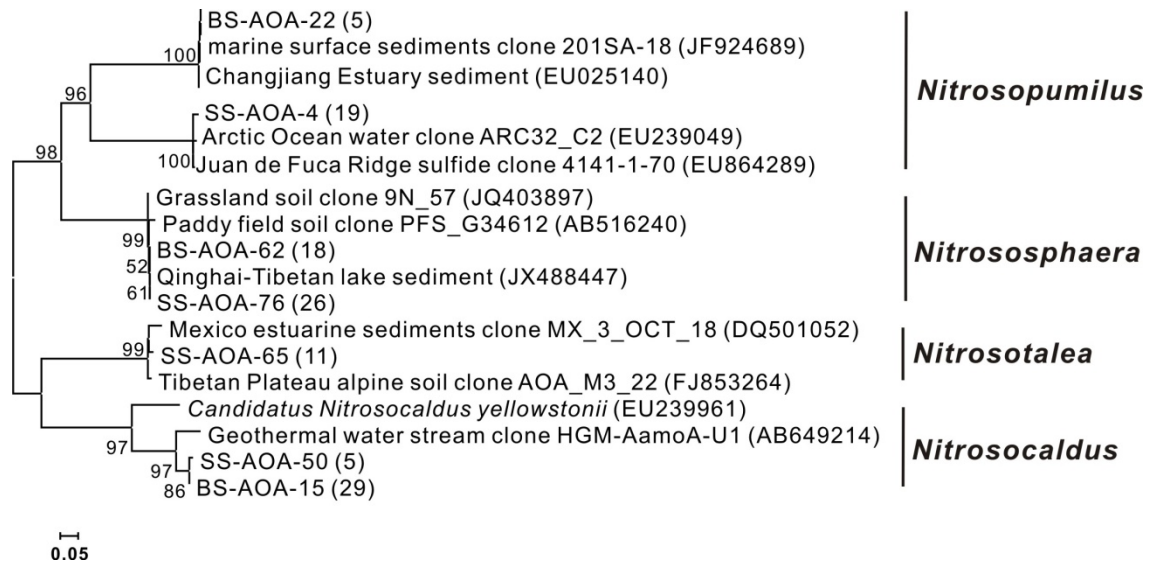
616 **Figure 4.** Archaeal phylogenetic tree based on 16S rRNA gene sequences, including various
 617 16S rRNA gene clones obtained from the Gongxiaoshe hot spring sediments (SS and BS) and
 618 cited some sequences from Hou et al. (2013) (stained by red). The tree is constructed using the
 619 neighbor-joining method, and bootstrap confidence values over 50% (1000 replicates) are
 620 shown. The scale bar represents the expected number of changes per nucleotide position.

621

622

623

624



625

626 **Figure 5.** The phylogenetic tree of archaeal amoA genes is cloned from the Gongxiaoshe hot
 627 spring sediments (SS and BS). The tree is constructed using the neighbor-joining method, and
 628 bootstrap confidence values over 50% (1000 replicates) are shown. The scale bar represents
 629 the expected number of changes per nucleotide position.

630